

VOL III

# THE GREAT WORLD OF NANOTECHNOLOGY

Emilio Castro Otero  
(Organizador)

 EDITORA  
ARTEMIS  
2025

VOL III

# THE GREAT WORLD OF NANOTECHNOLOGY

Emilio Castro Otero  
(Organizador)

 EDITORA  
ARTEMIS  
2025



O conteúdo deste livro está licenciado sob uma Licença de Atribuição Creative Commons Atribuição-Não-Comercial NãoDerivativos 4.0 Internacional (CC BY-NC-ND 4.0). Direitos para esta edição cedidos à Editora Artemis pelos autores. Permitido o download da obra e o compartilhamento, desde que sejam atribuídos créditos aos autores, e sem a possibilidade de alterá-la de nenhuma forma ou utilizá-la para fins comerciais.

A responsabilidade pelo conteúdo dos artigos e seus dados, em sua forma, correção e confiabilidade é exclusiva dos autores. A Editora Artemis, em seu compromisso de manter e aperfeiçoar a qualidade e confiabilidade dos trabalhos que publica, conduz a avaliação cega pelos pares de todos manuscritos publicados, com base em critérios de neutralidade e imparcialidade acadêmica.

<b>Editora Chefe</b>	Prof. <sup>a</sup> Dr. <sup>a</sup> Antonella Carvalho de Oliveira
<b>Editora Executiva</b>	M. <sup>a</sup> Viviane Carvalho Mocellin
<b>Direção de Arte</b>	M. <sup>a</sup> Bruna Bejarano
<b>Diagramação</b>	Elisangela Abreu
<b>Organizador</b>	Prof. Dr. Emilio Castro Otero
<b>Imagem da Capa</b>	yourapechkin/123RF
<b>Bibliotecário</b>	Maurício Amormino Júnior – CRB6/2422

#### Conselho Editorial

Prof.<sup>a</sup> Dr.<sup>a</sup> Ada Esther Portero Ricol, *Universidad Tecnológica de La Habana “José Antonio Echeverría”*, Cuba  
Prof. Dr. Adalberto de Paula Paranhos, *Universidade Federal de Uberlândia*, Brasil  
Prof. Dr. Agustín Olmos Cruz, *Universidad Autónoma del Estado de México*, México  
Prof.<sup>a</sup> Dr.<sup>a</sup> Amanda Ramalho de Freitas Brito, *Universidade Federal da Paraíba*, Brasil  
Prof.<sup>a</sup> Dr.<sup>a</sup> Ana Clara Monteverde, *Universidad de Buenos Aires*, Argentina  
Prof.<sup>a</sup> Dr.<sup>a</sup> Ana Júlia Viamonte, *Instituto Superior de Engenharia do Porto (ISEP)*, Portugal  
Prof. Dr. Ángel Mujica Sánchez, *Universidad Nacional del Altiplano*, Peru  
Prof.<sup>a</sup> Dr.<sup>a</sup> Angela Ester Mallmann Centenaro, *Universidade do Estado de Mato Grosso*, Brasil  
Prof.<sup>a</sup> Dr.<sup>a</sup> Begoña Blandón González, *Universidad de Sevilla*, Espanha  
Prof.<sup>a</sup> Dr.<sup>a</sup> Carmen Pimentel, *Universidade Federal Rural do Rio de Janeiro*, Brasil  
Prof.<sup>a</sup> Dr.<sup>a</sup> Catarina Castro, *Universidade Nova de Lisboa*, Portugal  
Prof.<sup>a</sup> Dr.<sup>a</sup> Cirila Cervera Delgado, *Universidad de Guanajuato*, México  
Prof.<sup>a</sup> Dr.<sup>a</sup> Cláudia Neves, *Universidade Aberta de Portugal*  
Prof.<sup>a</sup> Dr.<sup>a</sup> Cláudia Padovesi Fonseca, *Universidade de Brasília-DF*, Brasil  
Prof. Dr. Cleberton Correia Santos, *Universidade Federal da Grande Dourados*, Brasil  
Dr. Cristo Ernesto Yáñez León – *New Jersey Institute of Technology*, Newark, NJ, Estados Unidos  
Prof. Dr. David García-Martul, *Universidad Rey Juan Carlos de Madrid*, Espanha  
Prof.<sup>a</sup> Dr.<sup>a</sup> Deuzimar Costa Serra, *Universidade Estadual do Maranhão*, Brasil  
Prof.<sup>a</sup> Dr.<sup>a</sup> Dina Maria Martins Ferreira, *Universidade Estadual do Ceará*, Brasil  
Prof.<sup>a</sup> Dr.<sup>a</sup> Edith Luévano-Hipólito, *Universidad Autónoma de Nuevo León*, México  
Prof.<sup>a</sup> Dr.<sup>a</sup> Eduarda Maria Rocha Teles de Castro Coelho, *Universidade de Trás-os-Montes e Alto Douro*, Portugal  
Prof. Dr. Eduardo Eugênio Spers, *Universidade de São Paulo (USP)*, Brasil  
Prof. Dr. Eloi Martins Senhoras, *Universidade Federal de Roraima*, Brasil  
Prof.<sup>a</sup> Dr.<sup>a</sup> Elvira Laura Hernández Carballido, *Universidad Autónoma del Estado de Hidalgo*, México  
Prof.<sup>a</sup> Dr.<sup>a</sup> Emilas Darlene Carmen Lebus, *Universidad Nacional del Nordeste/ Universidad Tecnológica Nacional*, Argentina

Prof.<sup>a</sup> Dr.<sup>a</sup> Erla Mariela Morales Morgado, *Universidad de Salamanca*, Espanha  
 Prof. Dr. Ernesto Cristina, *Universidad de la República*, Uruguay  
 Prof. Dr. Ernesto Ramírez-Briones, *Universidad de Guadalajara*, México  
 Prof. Dr. Fernando Hitt, *Université du Québec à Montréal*, Canadá  
 Prof. Dr. Gabriel Díaz Cobos, *Universitat de Barcelona*, Espanha  
 Prof.<sup>a</sup> Dr.<sup>a</sup> Gabriela Gonçalves, Instituto Superior de Engenharia do Porto (ISEP), Portugal  
 Prof.<sup>a</sup> Dr.<sup>a</sup> Galina Gumovskaya – Higher School of Economics, Moscow, Russia  
 Prof. Dr. Geoffroy Roger Pointer Malpass, Universidade Federal do Triângulo Mineiro, Brasil  
 Prof.<sup>a</sup> Dr.<sup>a</sup> Gladys Esther Leoz, *Universidad Nacional de San Luis*, Argentina  
 Prof.<sup>a</sup> Dr.<sup>a</sup> Glória Beatriz Álvarez, *Universidad de Buenos Aires*, Argentina  
 Prof. Dr. Gonçalo Poeta Fernandes, Instituto Politécnico da Guarda, Portugal  
 Prof. Dr. Gustavo Adolfo Juarez, *Universidad Nacional de Catamarca*, Argentina  
 Prof. Dr. Guillermo Julián González-Pérez, *Universidad de Guadalajara*, México  
 Prof. Dr. Håkan Karlsson, *University of Gothenburg*, Suécia  
 Prof.<sup>a</sup> Dr.<sup>a</sup> Iara Lúcia Tescarollo Dias, Universidade São Francisco, Brasil  
 Prof.<sup>a</sup> Dr.<sup>a</sup> Isabel del Rosario Chiyon Carrasco, *Universidad de Piura*, Peru  
 Prof.<sup>a</sup> Dr.<sup>a</sup> Isabel Yohena, *Universidad de Buenos Aires*, Argentina  
 Prof. Dr. Ivan Amaro, Universidade do Estado do Rio de Janeiro, Brasil  
 Prof. Dr. Iván Ramon Sánchez Soto, *Universidad del Bío-Bío*, Chile  
 Prof.<sup>a</sup> Dr.<sup>a</sup> Ivânia Maria Carneiro Vieira, Universidade Federal do Amazonas, Brasil  
 Prof. Me. Javier Antonio Albornoz, *University of Miami and Miami Dade College*, Estados Unidos  
 Prof. Dr. Jesús Montero Martínez, *Universidad de Castilla - La Mancha*, Espanha  
 Prof. Dr. João Manuel Pereira Ramalho Serrano, Universidade de Évora, Portugal  
 Prof. Dr. Joaquim Júlio Almeida Júnior, UNIFIMES - Centro Universitário de Mineiros, Brasil  
 Prof. Dr. Jorge Ernesto Bartolucci, *Universidad Nacional Autónoma de México*, México  
 Prof. Dr. José Cortez Godínez, Universidad Autónoma de Baja California, México  
 Prof. Dr. Juan Carlos Cancino Díaz, Instituto Politécnico Nacional, México  
 Prof. Dr. Juan Carlos Mosquera Feijoo, *Universidad Politécnica de Madrid*, Espanha  
 Prof. Dr. Juan Diego Parra Valencia, *Instituto Tecnológico Metropolitano de Medellín*, Colômbia  
 Prof. Dr. Juan Manuel Sánchez-Yáñez, *Universidad Michoacana de San Nicolás de Hidalgo*, México  
 Prof. Dr. Juan Porras Pulido, *Universidad Nacional Autónoma de México*, México  
 Prof. Dr. Júlio César Ribeiro, Universidade Federal Rural do Rio de Janeiro, Brasil  
 Prof. Dr. Leinig Antonio Perazolli, Universidade Estadual Paulista (UNESP), Brasil  
 Prof.<sup>a</sup> Dr.<sup>a</sup> Livia do Carmo, Universidade Federal de Goiás, Brasil  
 Prof.<sup>a</sup> Dr.<sup>a</sup> Luciane Spanhol Bordignon, Universidade de Passo Fundo, Brasil  
 Prof. Dr. Luis Fernando González Beltrán, *Universidad Nacional Autónoma de México*, México  
 Prof. Dr. Luis Vicente Amador Muñoz, *Universidad Pablo de Olavide*, Espanha  
 Prof.<sup>a</sup> Dr.<sup>a</sup> Macarena Esteban Ibáñez, *Universidad Pablo de Olavide*, Espanha  
 Prof. Dr. Manuel Ramiro Rodríguez, *Universidad Santiago de Compostela*, Espanha  
 Prof. Dr. Manuel Simões, Faculdade de Engenharia da Universidade do Porto, Portugal  
 Prof.<sup>a</sup> Dr.<sup>a</sup> Márcia de Souza Luz Freitas, Universidade Federal de Itajubá, Brasil  
 Prof. Dr. Marcos Augusto de Lima Nobre, Universidade Estadual Paulista (UNESP), Brasil  
 Prof. Dr. Marcos Vinicius Meiado, Universidade Federal de Sergipe, Brasil  
 Prof.<sup>a</sup> Dr.<sup>a</sup> Mar Garrido Román, *Universidad de Granada*, Espanha  
 Prof.<sup>a</sup> Dr.<sup>a</sup> Margarida Márcia Fernandes Lima, Universidade Federal de Ouro Preto, Brasil  
 Prof.<sup>a</sup> Dr.<sup>a</sup> María Alejandra Arecco, *Universidad de Buenos Aires*, Argentina  
 Prof.<sup>a</sup> Dr.<sup>a</sup> Maria Aparecida José de Oliveira, Universidade Federal da Bahia, Brasil  
 Prof.<sup>a</sup> Dr.<sup>a</sup> Maria Carmen Pastor, *Universitat Jaume I*, Espanha  
 Prof.<sup>a</sup> Dr.<sup>a</sup> Maria da Luz Vale Dias – Universidade de Coimbra, Portugal  
 Prof.<sup>a</sup> Dr.<sup>a</sup> Maria do Céu Caetano, Universidade Nova de Lisboa, Portugal



Prof.<sup>ª</sup> Dr.<sup>ª</sup> Maria do Socorro Saraiva Pinheiro, Universidade Federal do Maranhão, Brasil  
 Prof.<sup>ª</sup> Dr.<sup>ª</sup> M<sup>ª</sup>Graça Pereira, Universidade do Minho, Portugal  
 Prof.<sup>ª</sup> Dr.<sup>ª</sup> Maria Gracinda Carvalho Teixeira, Universidade Federal Rural do Rio de Janeiro, Brasil  
 Prof.<sup>ª</sup> Dr.<sup>ª</sup> María Guadalupe Vega-López, *Universidad de Guadalajara, México*  
 Prof.<sup>ª</sup> Dr.<sup>ª</sup> Maria Lúcia Pato, Instituto Politécnico de Viseu, Portugal  
 Prof.<sup>ª</sup> Dr.<sup>ª</sup> Maritza González Moreno, *Universidad Tecnológica de La Habana, Cuba*  
 Prof.<sup>ª</sup> Dr.<sup>ª</sup> Maurícea Silva de Paula Vieira, Universidade Federal de Lavras, Brasil  
 Prof. Dr. Melchor Gómez Pérez, Universidad del Pais Vasco, Espanha  
 Prof.<sup>ª</sup> Dr.<sup>ª</sup> Ninfa María Rosas-García, Centro de Biotecnología Genómica-Instituto Politécnico Nacional, México  
 Prof.<sup>ª</sup> Dr.<sup>ª</sup> Odara Horta Boscolo, Universidade Federal Fluminense, Brasil  
 Prof. Dr. Osbaldo Turpo-Gebera, *Universidad Nacional de San Agustín de Arequipa, Peru*  
 Prof.<sup>ª</sup> Dr.<sup>ª</sup> Patrícia Vasconcelos Almeida, Universidade Federal de Lavras, Brasil  
 Prof.<sup>ª</sup> Dr.<sup>ª</sup> Paula Arcoverde Cavalcanti, Universidade do Estado da Bahia, Brasil  
 Prof. Dr. Rodrigo Marques de Almeida Guerra, Universidade Federal do Pará, Brasil  
 Prof. Dr. Saulo Cerqueira de Aguiar Soares, Universidade Federal do Piauí, Brasil  
 Prof. Dr. Sergio Bitencourt Araújo Barros, Universidade Federal do Piauí, Brasil  
 Prof. Dr. Sérgio Luiz do Amaral Moretti, Universidade Federal de Uberlândia, Brasil  
 Prof.<sup>ª</sup> Dr.<sup>ª</sup> Silvia Inés del Valle Navarro, *Universidad Nacional de Catamarca, Argentina*  
 Prof.<sup>ª</sup> Dr.<sup>ª</sup> Solange Kazumi Sakata, Instituto de Pesquisas Energéticas e Nucleares (IPEN)- USP, Brasil  
 Prof.<sup>ª</sup> Dr.<sup>ª</sup> Stanislava Kashtanova, *Saint Petersburg State University, Russia*  
 Prof.<sup>ª</sup> Dr.<sup>ª</sup> Susana Álvarez Otero – Universidad de Oviedo, Espanha  
 Prof.<sup>ª</sup> Dr.<sup>ª</sup> Teresa Cardoso, Universidade Aberta de Portugal  
 Prof.<sup>ª</sup> Dr.<sup>ª</sup> Teresa Monteiro Seixas, Universidade do Porto, Portugal  
 Prof. Dr. Valter Machado da Fonseca, Universidade Federal de Viçosa, Brasil  
 Prof.<sup>ª</sup> Dr.<sup>ª</sup> Vanessa Bordin Viera, Universidade Federal de Campina Grande, Brasil  
 Prof.<sup>ª</sup> Dr.<sup>ª</sup> Vera Lúcia Vasilévski dos Santos Araújo, Universidade Tecnológica Federal do Paraná, Brasil  
 Prof. Dr. Wilson Noé Garcés Aguilar, *Corporación Universitaria Autónoma del Cauca, Colômbia*  
 Prof. Dr. Xosé Somoza Medina, *Universidad de León, Espanha*

### **Dados Internacionais de Catalogação na Publicação (CIP) (eDOC BRASIL, Belo Horizonte/MG)**

O86g The Great World of Nanotechnology III / organização de Emilio Castro Otero. – 1. ed. – Curitiba, PR : Editora Artemis, 2025.

Formato: PDF

Requisitos de sistema: Adobe Acrobat Reader

Modo de acesso: World Wide Web

Edição bilingue.

Inclui bibliografia

ISBN 978-65-81701-79-6

DOI 10.37572/EdArt\_121225796

1. Nanotecnologia biomédica. 2. Engenharia de tecidos. 3. Nanomateriais – Aplicações. 4. Biosistemas – Inovação tecnológica. 5. Sensores avançados – Desenvolvimento. I. Otero, Emilio Castro.

CDD 620.5

**Elaborado por Maurício Amormino Júnior – CRB6/2422**



## FOREWORD

We are thrilled to present the third installment of ***The Great World of Nanotechnology***, a volume dedicated to exploring the cutting edge of nanotechnology applications, from the fundamental science of materials to their tangible impact on health, industry, and the environment. This book is meticulously structured into four thematic blocks, designed to guide the reader through the latest innovations that seek to solve crucial challenges in modern society.

The first pillar of this volume, ***Fundamentals of Nanomaterial Manufacturing and Characterization***, delves into the critical methodologies for creating high-quality nanostructures. Chapter 1 offers systematic research on the Effects of the Transfer Process on the Structure of Graphene Synthesized by Chemical Vapor Deposition. Complementing this, Chapter 2 examines Polymer Nanofibers via Airbrushing.

In ***Nanomaterials for Surface Engineering and Smart Sensors***, the chapters explore how these nanostructures can be applied in functional devices and material protection. Chapter 3 presents advances in the development of sensors based on graphene functionalized with nanoparticles. Similarly, Chapter 4 addresses the electrodeposition of nanostructured metal coatings.

***Nanotechnology in Biomedical and Pharmaceutical Applications*** brings three chapters focusing on the use of nanotechnology to improve human health. Chapter 5 evaluates the Cytotoxic Effect of Nanoemulsion with Pumpkin Seed Oil on Breast Cancer Cell Lines. In the field of tissue engineering, Chapter 6 describes the development of Alginate/Collagen Structures Enhanced with Conductive Nanoparticles (PEDOT) for the Regeneration of Small-Diameter Blood Vessels. Finally, Chapter 7 discusses the development of an antiseptic gel based on bioactive compounds encapsulated in nanoparticles.

Concluding our exploration, ***Nanotechnological Solutions for Environmental Remediation*** addresses the water pollution crisis. The final chapter describes the Removal of Arsenic from Groundwater Using Recycled Iron Nanoparticles through the development of a low-cost filter that uses iron nanoparticles.

We invite you to immerse yourself in reading *The Great World of Nanotechnology*. Vol. III, where science on the smallest scale translates into large-scale solutions. We sincerely hope that this compilation of advanced research will not only be of utmost interest to you, but also inspire new directions of study and application in this infinitely promising field.

Emilio Castro Otero

## PRÓLOGO

É com grande entusiasmo que apresentamos a terceira edição de ***The Great World of Nanotechnology***, um volume dedicado a explorar a vanguarda das aplicações nanotecnológicas, desde a ciência fundamental dos materiais até o seu impacto tangível na saúde, na indústria e no ambiente. Este livro está meticulosamente estruturado em quatro eixos temáticos, concebidos para guiar o leitor através das mais recentes inovações que procuram resolver desafios cruciais na sociedade moderna.

O primeiro eixo deste volume, ***Fundamentos da Fabricação e Caracterização de Nanomateriais***, aprofunda as metodologias críticas para a criação de nanoestruturas de alta qualidade. O Capítulo 1 oferece uma investigação sistemática sobre os Efeitos do Processo de Transferência na Estrutura do Grafeno Sintetizado por Deposição Química de Vapor e o segundo capítulo examina as Nanofibras Poliméricas via Aerografia.

Em seguida, o eixo ***Nanomateriais para Engenharia de Superfícies e Sensores Inteligentes***, explora como essas nanoestruturas podem ser aplicadas em dispositivos funcionais e proteção de materiais. O Capítulo 3 apresenta os avanços no desenvolvimento de Sensores Baseados em Grafeno Funcionalizado com Nanopartículas. Paralelamente, e o Capítulo 4 aborda a Eletrodeposição de Revestimentos Metálicos Nanoestruturados.

O eixo ***Nanotecnologia em Aplicações Biomédicas e Farmacêuticas***, centra-se na utilização da nanotecnologia para melhorar a saúde humana. O Capítulo 5 avalia o Efeito Citotóxico da Nanoemulsão com Óleo de Semente de Abóbora em Linhagens de Células de Cancro da Mama. No campo da engenharia de tecidos, o Capítulo 6 descreve o desenvolvimento de Estruturas de Alginato/Colagénio Melhoradas com Nanopartículas Condutoras (PEDOT) para a regeneração de Vasos Sanguíneos de Pequeno Diâmetro. Finalmente, o Capítulo 7 expõe a Elaboração de um Gel Antisséptico Baseado em Compostos Bioativos Encapsulados em Nanopartículas.

Concluindo a nossa exploração, o eixo ***Soluções Nanotecnológicas para Remédios Ambientais***, aborda a crise da contaminação da água. Este último capítulo descreve a Eliminação de Arsénico das Águas Subterrâneas Usando Nanopartículas de Ferro Reciclado, através do desenvolvimento de um filtro de baixo custo que utiliza nanopartículas de ferro.

Convidamo-lo a mergulhar na leitura de *The Great World of Nanotechnology Vol. III*, onde a ciência na escala mais pequena se traduz em soluções em grande escala. Esperamos sinceramente que esta compilação de pesquisas avançadas não só seja do seu interesse, mas também inspire novos rumos de estudo e aplicação neste campo infinitamente promissor.

Emilio Castro Otero

TABLE OF CONTENTS

FUNDAMENTALS OF NANOMATERIAL MANUFACTURING AND CHARACTERIZATION

CHAPTER 1..... 1

EFFECTS OF THE TRANSFER PROCESS ON THE STRUCTURE OF CVD-SYNTHESIZED GRAPHENE: A RAMAN SPECTROSCOPY STUDY


Rodrigo Segura-del-Río  
Fernanda Olivares Salgado  
Ricardo Henríquez Correa

 [https://doi.org/10.37572/EdArt\\_1212257961](https://doi.org/10.37572/EdArt_1212257961)

CHAPTER 2..... 15

NANOFIBRAS POLIMÉRICAS POR FIAÇÃO POR SOPRO EM SOLUÇÃO VIA AEROGRAFIA: UMA REVISÃO DAS PROPRIEDADES, VANTAGENS TECNOLÓGICAS E APLICAÇÕES EMERGENTES

Gabriel da Cruz Dias  
Thelma Sley Pacheco Cellet  
Mirian Cristina dos Santos  
Caroline Silva Danna  
Paulo Roberto Orlandi Ruiz  
Deuber Lincon Agostini da Silva  
Clarissa de Almeida Olivati

 [https://doi.org/10.37572/EdArt\\_1212257962](https://doi.org/10.37572/EdArt_1212257962)

NANOMATERIALS FOR SURFACE ENGINEERING AND SMART SENSORS

CHAPTER 3..... 34

SENSORES BASADOS EN GRAFENO FUNCIONALIZADO CON PT-SN/TIO<sub>2</sub> PARA DETECCIÓN DE SO<sub>2</sub>

Luz María García-Rivera  
Juan Manuel Padilla Flores  
Octavio Maldonado Saavedra  
Erick A. Juarez-Arellano

 [https://doi.org/10.37572/EdArt\\_1212257963](https://doi.org/10.37572/EdArt_1212257963)



## **CHAPTER 4..... 50**

### **ELECTRODEPOSICIÓN DE RECUBRIMIENTOS METÁLICOS NANOESTRUCTURADOS**

Marcos Bedolla Hernández

Genaro Texcucano Romano

Jorge Bedolla Hernández

Jorge Aguilar Vázquez

Carlos Alberto Mora Santos

Luz Fabiola Sánchez Parra

 [https://doi.org/10.37572/EdArt\\_1212257964](https://doi.org/10.37572/EdArt_1212257964)

## **NANOTECHNOLOGY IN BIOMEDICAL AND PHARMACEUTICAL APPLICATIONS**

## **CHAPTER 5..... 60**

### **CYTOTOXIC EFFECT OF PUMPKIN SEED OIL-LOADED NANOEMULSION IN BREAST CANCER CELL LINES**

Anelise Pereira Alves

Wanderleya Toledo dos Santos

Daniel Augusto de Andrade

Felipe Kelmer Müller

Kézia Cristine Barbosa Ferreira

Guilherme Diniz Tavares

Fabiano Freire Costa

Paula Rocha Chellini

Ana Cláudia Chagas de Paula

 [https://doi.org/10.37572/EdArt\\_1212257965](https://doi.org/10.37572/EdArt_1212257965)

## **CHAPTER 6..... 74**

### **ENHANCED ALGINATE/COLLAGEN SCAFFOLDS WITH CONDUCTIVE POLY (3,4-ETHYLENEDIOXYTHIOPHENE) NANOPARTICLES FOR NEXT-GENERATION SMALL-DIAMETER TISSUE-ENGINEERED BLOOD VESSELS**

Emilio Castro

Èlia Bosch-Rué

Sara Estruch-Sotoca

Román A. Pérez

 [https://doi.org/10.37572/EdArt\\_1212257966](https://doi.org/10.37572/EdArt_1212257966)

**CHAPTER 7 ..... 86**

ELABORATION OF AN ANTISEPTIC GEL BASED ON BIOACTIVE COMPOUNDS  
OF *ORIGANUM VULGARE* AND *ALOE VERA* ENCAPSULATED IN  $\text{SiO}_2$  Y  $\text{ZNO-SNO}_2$   
NANOPARTICLES FOR CONTROLLED RELEASE

Guadalupe Luna Cedillo  
Francisco Javier Tzompantzi Morales  
Sandra Luz Hernández-Valladolid  
Juan Manuel Padilla Flores

 [https://doi.org/10.37572/EdArt\\_1212257967](https://doi.org/10.37572/EdArt_1212257967)

**NANOTECHNOLOGICAL SOLUTIONS FOR ENVIRONMENTAL REMEDIATION**

**CHAPTER 8 ..... 96**

ARSENIC REMOVAL FROM GROUNDWATER USING RECYCLED IRON  
NANOPARTICLES: DEVELOPMENT AND EVALUATION OF A LOW-COST FILTER FOR  
RURAL COMMUNITIES

Juan Simón Torres Espada  
Yrene Romina Lazcano Cruz

 [https://doi.org/10.37572/EdArt\\_1212257968](https://doi.org/10.37572/EdArt_1212257968)

**ABOUT THE ORGANIZER ..... 106**

**INDEX ..... 107**

# CHAPTER 1

## EFFECTS OF THE TRANSFER PROCESS ON THE STRUCTURE OF CVD-SYNTHESIZED GRAPHENE: A RAMAN SPECTROSCOPY STUDY

*Data de submissão: 10/11/2025*

*Data de aceite: 24/11/2025*

**Rodrigo Segura-del-Río**

Instituto de Química  
Facultad de Ciencias  
Universidad de Valparaíso  
Valparaíso, Chile  
<https://orcid.org/0000-0003-0928-0021>

**Fernanda Olivares Salgado**

Departamento de Física, Universidad Técnica  
Federico Santa María  
Valparaíso, Chile  
<https://orcid.org/0000-0002-9727-0677>

**Ricardo Henríquez Correa**

Departamento de Física, Universidad Técnica  
Federico Santa María  
Valparaíso, Chile  
<https://orcid.org/0000-0001-5141-1676>

**ABSTRACT:** In this chapter, a systematic investigation about the synthesis and transfer of graphene through the chemical vapor deposition (CVD) of methane ( $\text{CH}_4$ ) and acetylene ( $\text{C}_2\text{H}_2$ ) as the carbon precursors onto copper substrates is provided. Raman spectroscopy enabled the characterization of the number of layers, the level of disorder and the structural changes created by the transfer process to the silicon substrates. The

findings indicate that  $\text{CH}_4$  has more favorable effect on the growth of graphene films with reduced defect density and higher control of thickness than  $\text{C}_2\text{H}_2$ . Also, it was found out that the transfer creates effective reduction in the number of layers and changes in the relative intensities of the D, G and 2D bands, which is due to strain effects, interaction with the support polymer, and support polymer residues. These findings aid in shedding light on the processes that influence the mechanism of maintaining structural integrity of graphene in its processing and give a guideline to the manufacturing production of high-quality films to be used in electronic and photoelectrocatalytic tasks.

**KEYWORDS:** graphene; chemical vapor deposition; raman spectroscopy; graphene transfer.

### 1. INTRODUCTION

Graphene is a two-dimensional allotrope of carbon, formed by atoms arranged in a hexagonal network of only one atom in thickness. Since its isolation by Geim and Novoselov in 2004, research related to this material has increased drastically, and its relevance was recognized with the Nobel Prize in Physics in 2010. The electronic, thermal, and mechanical properties of graphene make it a material of high scientific and technological

interest. It stands out for its exceptional electrical conductivity (Martini et al., 2019), derived from its structure of  $sp^2$  covalent bonds and delocalized  $\pi$  electrons, and for its high thermal conductivity, estimated between 3000 and 5000  $W \cdot m^{-1} \cdot K^{-1}$  (Ghosh et al., 2010), values that suggest that graphene conducts heat better than carbon nanotubes (Balandin et al., 2008). Its elastic modulus reaches 42  $N \cdot m^{-1}$ , with a mechanical deformation of approximately 25% before breaking (Lee et al., 2008). Other significant properties are its large surface area (Liu et al., 2019) and its transparency (Nair et al., 2008). However, all these properties can vary significantly depending on the synthesis technique and the precursor used.

The techniques for obtaining graphene are divided into two main categories (Olabi et al., 2021). The first category includes methods in which graphite is used as the raw material. This category is called “top-down,” which means “from top to bottom”. In this category three methods can be distinguished, which are mechanical exfoliation (Gao et al., 2018), chemical exfoliation (Kamedulski et al., 2019), and chemical synthesis (Liu et al., 2008), the latter including the reduction of graphene oxide. From the exfoliation of graphite, a powder composed of graphene flakes is obtained, which is very convenient for experimental use in laboratories and for large-scale applications. The general limitation of these methods is that it is very difficult to obtain large-area material. In general, exfoliation methods starting from graphite are the simplest; however, during the process many defects are generated in the graphene sheets. Although defects can serve as active sites for electrochemical reactions, they also considerably decrease the performance of graphene’s most notable properties, which are electrical and thermal conduction. The second category includes all methods in which a carbon source is used as a molecular or atomic precursor to generate graphene growth. This category is called “bottom-up,” which means “from bottom to top,” in the sense that graphene is built from atoms or small molecular fragments. The methods included in this section are pyrolysis (Karu et al., 1966), epitaxial growth (First et al., 2010), and CVD (Wei et al., 2009). Through epitaxial growth on SiC, high-quality graphene can be obtained. The two main drawbacks of this method are the high cost of SiC wafers and the high synthesis temperatures above 1000 °C. On the other hand, graphene synthesized by pyrolysis has a low cost and a highly pure material can be obtained. However, the number of defects observed in the graphene is high, so the properties of the material are not optimal. Finally, the CVD technique is the most convenient in terms of quality and price (Novoselov et al., 2012).

It is important to highlight that in the CVD technique any carbon source in solid, liquid, or gaseous state can be used as a synthesis precursor. But the most significant advantage compared to other techniques is that it allows controlling the number of

graphene layers by adjusting parameters such as temperature and synthesis time, and the amount of precursor. The number of graphene layers is one of the most important characteristics of this material, since, as mentioned earlier, the properties vary significantly between a monolayer and multilayer graphene. In addition, the presence of  $H_2$  also plays an important role in the synthesis. Graphene can grow without  $H_2$ ; however, this molecule has a catalytic effect that affects the growth mechanism (Qi et al., 2013).

On the other hand, the synthesis substrate plays a fundamental role in graphene growth. The most used substrates are transition metals such as nickel (Ni) (Yu et al., 2008), platinum (Pt), palladium (Pd) (Kwon et al., 2009), iridium (Ir) (Coraux et al., 2009), and copper (Cu) (Song et al., 2014). The disadvantage of Ni is the high percentage of carbon solubility. The solubility of carbon in the substrate must be optimal so that it is not difficult to transfer it to another substrate later. In addition, Ni is limited by its small grain size. This is important because, with larger grain size, the synthesized graphene exhibits larger areas without boundaries that can act as defects. On the other hand, substrates such as Pt, Pd, and Ir are quite costly. Cu is the best option currently because it has lower carbon solubility compared to Ni and a much lower cost than other transition metals (Zhang et al., 2011). In addition, its grain size can be increased through an annealing process. These characteristics make it possible to transfer graphene more easily from Cu than from other substrates (Li et al., 2009).

Finally, the synthesis precursor is very important, since the decomposition mechanism and subsequent formation of graphene vary depending on the chosen precursor molecule. The most used precursor is methane ( $CH_4$ ). The decomposition mechanism of this molecule to form graphene has been described as successive dehydrogenation stages (Zhang et al., 2011). Another carbon source that can be used is acetylene ( $C_2H_2$ ). This precursor is promising because it produces rapid graphene growth. In addition, it is possible to control the number of layers by adjusting the injection time with the CVD technique (Song et al., 2014). Graphene can grow without  $H_2$ ; however, some authors indicate that it promotes the process with a catalytic effect. The properties of graphene and its atomic structure make it an ideal platform for synthesizing other carbon materials or materials of different nature. Graphene could improve the efficiency and durability of many applications. However, it is necessary to critically address its current limitations.

## 2. GRAPHENE SYNTHESIS AND TRANSFER

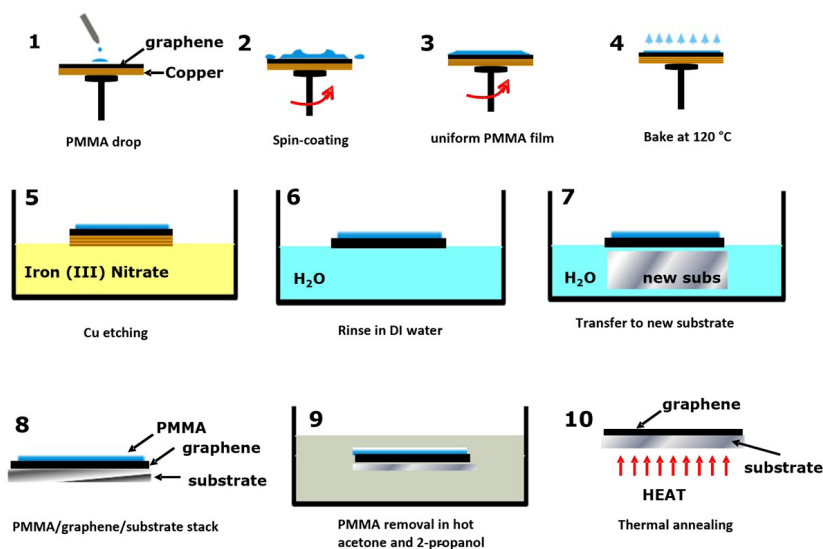
Graphene was synthesized on copper foils of  $2.25\text{ cm}^2$  (MTI, purity > 99.99%, thickness  $25\text{ }\mu\text{m}$ ), previously cleaned by ultrasound in ethanol and acetone for 5 min with



each solvent (Song et al., 2014; Segura et al., 2016). The CVD process was carried out in three stages. First, the substrate was annealed at the synthesis temperature for 20 min under a flow of 200 sccm of Ar/H<sub>2</sub> to increase the grain size of the Cu. Then, in the growth stage, the carbon precursor (CH<sub>4</sub> or C<sub>2</sub>H<sub>2</sub>) was injected with a constant flow of 2 sccm for variable intervals of 1 to 30 min, maintaining 200 sccm of Ar and adjusting the amount of H<sub>2</sub> between 0 and 100 sccm. Finally, the system was cooled to room temperature under Ar flow. To optimize the synthesis conditions, four fundamental parameters were evaluated: (i) deposition time (1–30 min), (ii) temperature (950, 1000, and 1050 °C), (iii) H<sub>2</sub> flow (0, 5, and 20 sccm), and (iv) precursor flow (1–10 sccm). The comparison between methane and acetylene allowed establishing their influence on the quality, number of layers, and uniformity of the graphene.

Subsequently, the graphene was transferred from the copper to the final substrate using a method assisted by polymethyl methacrylate (PMMA) (Suk et al., 2011). A total of 90 µL of a PMMA solution (20 mg/mL in chlorobenzene) was applied by spin-coating at 500 rpm for 10 s and 1500 rpm for 50 s, followed by curing at 120 °C for 5 min. The Cu was dissolved in an aqueous solution of Fe(NO<sub>3</sub>)<sub>3</sub> 1 M until complete removal, and the PMMA/graphene film was washed three times with distilled water. It was then transferred onto the new substrate and dried under vacuum for 2 h, followed by heating at 180 °C for 30 min. The polymer was removed by successive immersion in acetone (40 °C, 3 min) and 2-propanol (3 min), finishing with a thermal treatment at 400 °C under Ar/H<sub>2</sub> flow. The complete transfer procedure is shown schematically in Figure 1.

Figure 1. Schematic of the graphene transfer process.



### 3. RESULTS

The synthesis of graphene on copper was optimized by CVD using two carbon precursors, acetylene and methane. For both, four main parameters were evaluated: (i) deposition time (1–30 min), (ii) temperature (950, 1000, and 1050 °C), (iii) hydrogen flow (0–100 sccm), and (iv) precursor flow (2–10 sccm).

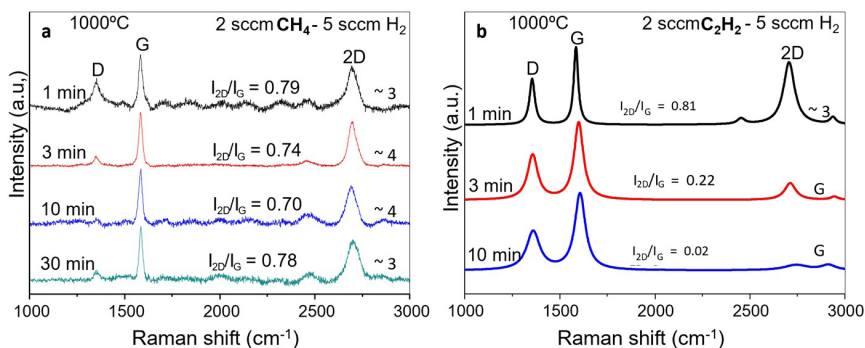
The samples were characterized by Raman spectroscopy using a Renishaw inVia spectrometer with a 532 nm laser, to determine the number of layers and the degree of structural disorder. A 25× objective was used, and the laser intensity was kept at 5%. Ten spectra were collected from different regions of each sample and averaged, providing statistically representative data and minimizing the influence of local inhomogeneities or measurement artifacts. This technique is widely used to evaluate the quality of graphene, since it allows rapid and non-destructive identification of the number of layers, defects, and strain in the lattice (Saito et al., 2011; Pimenta et al., 2008). In the Raman spectra of graphene, the main bands distinguished are the D band ( $\sim 1350\text{ cm}^{-1}$ ), G band ( $\sim 1580\text{ cm}^{-1}$ ), and 2D band ( $\sim 2690\text{ cm}^{-1}$ ), occasionally accompanied by secondary signals such as D' ( $1620\text{ cm}^{-1}$ ), G<sup>+</sup> ( $2450\text{ cm}^{-1}$ ), and D+G ( $2940\text{ cm}^{-1}$ ). The D band is associated with defects or grain boundaries and does not appear in pristine graphene. Its intensity increases with the defect density. The G band, originating from an in-plane vibrational mode (iTO and LO), is present in all types of graphene and its position is sensitive to strain or doping. The 2D band, corresponding to a second-order double-resonance process, is particularly useful for determining the number of layers: its shape and intensity change systematically with interlayer interaction (Malard et al., 2009). As the number of layers increases, the 2D band broadens and loses intensity, while the G band undergoes a slight shift to lower frequencies. In single-layer graphene, the 2D band is intense, symmetric, and narrow, with an  $I_{2D}/I_G$  intensity ratio  $> 2$ ; in bilayers and few-layer graphene this value decreases progressively. Therefore, the  $I_{2D}/I_G$  ratio constitutes a direct criterion to estimate the number of layers and the structural quality of the material. The appearance and shape of the defect-induced bands (D, D', and D+G) also allow evaluation of the degree of crystalline order. In highly defective materials the D band increases notably, while in high-quality graphene this band is weak or absent. Raman spectroscopy offers an unequivocal, rapid, and non-destructive identification of single-layer, bilayer, and multilayer graphene, and is currently the most widely used method to characterize graphene (Ferrari et al., 2006; Ni et al., 2008). In this study, correlating the Raman response with the synthesis parameters enabled the

determination of optimal conditions for producing few-layer, low-defect graphene on copper. The following section presents the results obtained from this optimization.

### 3.1. EFFECT OF SYNTHESIS TIME

To analyze the effect caused by the precursor injection time, all fabrication parameters were kept constant while varying the time between 1 and 30 minutes, for the two proposed carbon sources ( $\text{CH}_4$  and  $\text{C}_2\text{H}_2$ ). The synthesis temperature used was  $1000^\circ\text{C}$ , the precursor flow 2 sccm, and the hydrogen flow 5 sccm. In Figure 2a, the Raman spectra for the samples prepared with  $\text{CH}_4$  are presented. In this case, the ratio between the intensities of the 2D and G bands ( $I_{2D}/I_G$ ) varies between 0.70 and 0.80, which corresponds approximately to 3 or 4 layers of graphene (Song et al., 2014). Despite increasing the time from 1 to 30 minutes, no significant difference is observed in the number of layers. Where a difference can be noticed is in the intensity of the D band. As the synthesis time increases, the intensity of this band decreases, which indicates a decrease in the number of defects. It is possible that by increasing the synthesis time, the molecules manage to form larger areas of material, and therefore the sample presents fewer grain boundaries and better-finished hexagonal structures. Therefore, in this case it is favorable to increase the synthesis time and obtain graphene sheets with better crystalline properties. On the other hand, in Figure 2b it can be noticed that in comparison with the syntheses performed with  $\text{CH}_4$ , the samples prepared with  $\text{C}_2\text{H}_2$  do show an important difference when modifying the synthesis time. The 1-minute synthesis presents an  $I_{2D}/I_G$  ratio of 0.81, which corresponds approximately to 3 layers of graphene. Meanwhile, the 3- and 10-minute syntheses present ratios of 0.22 and 0.02 respectively, values that correspond to the formation of graphite.

Figure 2. Raman spectra for the graphene syntheses carried out by varying the precursor injection time a) methane and b) acetylene.

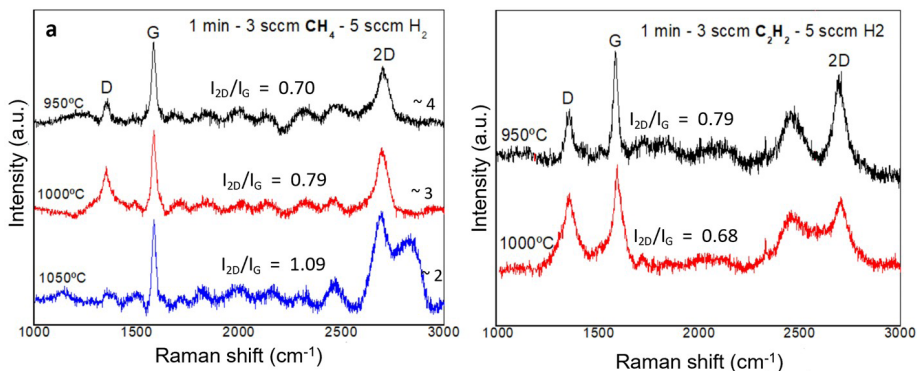


The difference observed between both precursors can be explained based on the molecular structure. It had previously been reported that  $C_2H_2$  is a promising raw material because it produces a rapid growth of the graphene layers (Song et al., 2014). This makes sense if we consider that the  $CH_4$  molecule has only one carbon atom, so it must join with another 5 carbon atoms to form a hexagon and break 4 C–H bonds to form the graphitic structure. On the other hand,  $C_2H_2$  has two carbon atoms in its structure, so from 3 molecules a graphene hexagon can be formed. Under this context it is coherent that when increasing the synthesis time with  $CH_4$  from 1 to 30 minutes practically the same number of layers is formed, while when using  $C_2H_2$  the number of layers increases drastically.

### 3.2. EFFECT OF SYNTHESIS TEMPERATURE

In this section the effect of temperature on the synthesis of graphene was analyzed, keeping constant the other three parameters studied, which are the time, precursor flow, and hydrogen flow, for both  $CH_4$  and  $C_2H_2$ . The synthesis time selected was 1 minute, and the precursor and hydrogen flow used was 3 and 5 sccm respectively. In Figure 3a the Raman spectra is presented for the samples prepared using  $CH_4$ . In this case, graphene of 4, 3, and 2 layers were obtained when the synthesis was carried out at 950 °C, 1000 °C, and 1050 °C respectively. That is, when increasing the synthesis temperature, the number of graphene layers decreases under the mentioned conditions. On the contrary, as can be seen in Figure 3b, when the synthesis is carried out with  $C_2H_2$ , the number of graphene layers increases when the temperature increases. Graphene of 3 and 5 layers was obtained when the synthesis temperature increased from 950 to 1000 °C.

Figure 3. Raman spectra for the graphene syntheses carried out with a) methane and b) acetylene for different synthesis temperatures.

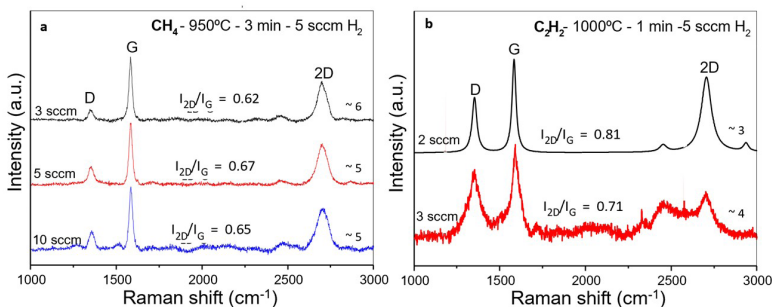


Again, in this section completely opposite phenomena are observed when comparing the two precursors. When increasing the synthesis temperature, the number of layers decreases if  $\text{CH}_4$  is used and increases if  $\text{C}_2\text{H}_2$  is used. It can also be observed that in the syntheses carried out with acetylene the intensity of the D band is higher, which indicates that the graphene sheets have more defects.

### 3.3. EFFECT OF PRECURSOR FLOW

To understand how the amount of precursor ( $\text{CH}_4$  and  $\text{C}_2\text{H}_2$ ) added in the synthesis of graphene affects the material, the synthesis time, temperature, and amount of hydrogen were kept constant. In Figure 4a the Raman spectra is presented for the samples synthesized with  $\text{CH}_4$ . For this precursor the injection flows selected were 3, 5, and 10 sccm. In the 3 spectra the ratio between the intensities of the  $I_{2D}/I_G$  bands varies around 0.60, which corresponds to approximately 5 or 6 layers of graphene. That is, when increasing the amount of precursor between 3 and 10 sccm it is not possible to notice a substantial difference in the number of layers. The D band also does not show significant changes in its intensity, and the presence of the other two disorder-related bands (D' and D+G) is not appreciated. On the contrary, when using  $\text{C}_2\text{H}_2$  as precursor a drastic variation occurs when increasing its injection flow. As can be seen in Figure 4b, when increasing the flow from 2 to 3 sccm only, the  $I_{2D}/I_G$  ratio varies from 0.81 to 0.71, that is, it increases from 3 to 4 layers with only 1 sccm difference. The above indicates that it is much more difficult to control the growth of this material using acetylene. On the other hand, it is also observed at first sight that the D band is much more intense in comparison with the spectra of the samples prepared with methane. In addition, the presence of another band produced by disorder, which is the D+G band, is observed. This indicates that the samples prepared with  $\text{C}_2\text{H}_2$  present a greater number of defects than those prepared with  $\text{CH}_4$ . It is worth noting that the G+ band also appears to the left of the 2D band. However, in the literature there is still no clear consensus about the appearance of this band.

Figure 4. Raman spectra for the graphene syntheses with different amounts of flow of: a) methane and b) acetylene.



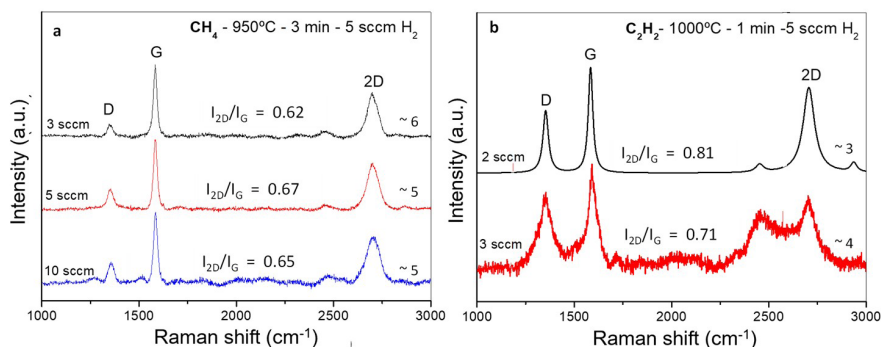


### 3.4. EFFECT OF HYDROGEN FLOW

In this section the effect of the hydrogen present in the synthesis of graphene was analyzed. The time, temperature, and precursor flow were kept constant. When analyzing how the amount of hydrogen affects the syntheses carried out with  $\text{CH}_4$ , it was found that with a lower amount of hydrogen a lower number of graphene layers is generated. As can be seen in Figure 5a, the synthesis prepared with 20 sccm of  $\text{H}_2$  presents an  $I_{2D}/I_G$  ratio of 0.50, which corresponds to more than 8 layers. Meanwhile, the graphene synthesized without  $\text{H}_2$  presents approximately 3 layers. In this case, if the objective is to obtain few-layer graphene, the most appropriate is to prepare it without  $\text{H}_2$ . However, it is probable that this graphene has a greater number of small grains. Hydrogen performs at least two functions in this synthesis (Vlassiuk et al., 2011). First, it acts as a catalyst for the activation of carbon through the dehydrogenation of methane and also participates in the control of grain size. This means that the presence of hydrogen allows the formation of larger grains, which improves the conductive properties of the material.

Similar to the synthesis carried out with  $\text{CH}_4$ , the syntheses carried out with  $\text{C}_2\text{H}_2$  present a lower number of layers when decreasing the amount of hydrogen injected (Figure 5b). When adding 20 sccm of  $\text{H}_2$  an  $I_{2D}/I_G$  ratio of 0.68 was obtained. Meanwhile, when adding 5 sccm of  $\text{H}_2$  the  $I_{2D}/I_G$  ratio increases to 0.81 and consequently the number of layers decreases.

Figure 5. Raman spectra of graphene obtained using a) methane and b) acetylene with different amounts of hydrogen.



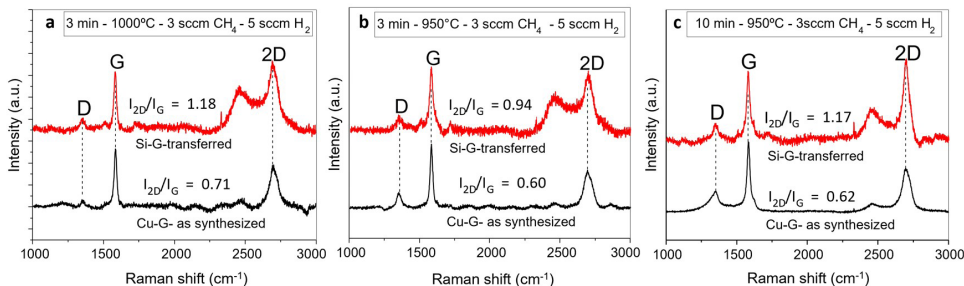
### 3.5. GRAPHENE TRANSFER AND SELECTION OF SYNTHESIS PARAMETERS

In this section the results obtained for the optimization of the transfer of graphene from the synthesis substrate (copper) to a new substrate are presented. For this study silicon was used as the transfer substrate and the procedure described previously

was employed. The analysis revealed that, when transferring the graphene samples, they undergo a kind of exfoliation during the process, as a result of the adhesion and release of the sheet on different surfaces until its final deposition. For this reason, when comparing the Raman spectra of graphene on copper and then on silicon, an increase in the  $I_{2D}/I_G$  ratio is observed, indicating a decrease in the number of layers (Figure 6). It is worth noting that, after the study of the synthesis of graphene, the optimal precursor and parameters were selected to facilitate the transfer and preserve its properties. As the optimal precursor  $CH_4$  was chosen, since with  $C_2H_2$  it is much more difficult to control the number of layers: small variations in its parameters completely modify the results. In contrast, with methane it is easier to maintain precise control of the thickness and reduce the number of structural defects. With respect to the synthesis parameters, these were selected considering the decrease in the number of layers that is produced by the exfoliation that the samples mentioned previously undergo. It was observed that, if in the synthesis graphene between 4 and 6 layers is obtained, which corresponds to an  $I_{2D}/I_G$  ratio between 0.60 and 0.70, then after the transfer the graphene presents 2 layers, as can be seen in Figure 6. Figure 6 shows 3 spectra of graphene synthesized on copper (black line) and also 3 spectra of the same graphene samples after the transfer onto silicon (red line). In Figure 6a the Raman spectra can be observed for a sample prepared for 3 minutes at 1000 °C. This sample on copper presented an  $I_{2D}/I_G$  ratio of 0.71 and then on silicon a ratio of 1.18. Initially the synthesized sample presented approximately 4 layers and after the transfer presents 2 layers. It is worth noting that when the  $I_{2D}/I_G$  ratio is close to 1, this corresponds to a graphene bilayer since both bands are equal. Meanwhile, in a spectrum of a monolayer of graphene the 2D band can be between 2 and 4 times larger than the G band. That is, the ratio between the intensities of these bands can also be between 2 and 4. In Figure 6b something very similar is observed. The graphene sample was prepared for 3 minutes at 950 °C. In this case the ratio between the intensities of the  $I_{2D}/I_G$  bands varies from 0.60 to 0.94. In number of layers these values correspond to 4–5 layers synthesized and 2 layers after the transfer. Then, in Figure 6c the spectrum can be observed for a sample prepared for 10 minutes at 950 °C. The ratio between the  $I_{2D}/I_G$  bands is 0.62 in the synthesis and 1.17 in the transfer. As in Figures 6a and 6b, in the synthesis approximately 5 layers are observed and then the transferred material corresponds to a graphene bilayer. An important difference observed when comparing all the spectra of the synthesized graphene with the transferred graphene is the increase of the  $G^+$  band, which as mentioned previously appears at approximately 2450  $cm^{-1}$  (Shimada et al., 2005). The origin of this band has been explained from different hypotheses by various authors which have been refuted over the years (Malard et al., 2009). Currently

there is still controversy about the assignment of this band (Saito et al., 2011). The reason is that there are different Raman DR (double resonance) components that occur at the same frequency, and it is still not clear which of them is responsible for the formation of this peak. On the contrary, the relative intensity of the Raman features associated with defects (for example, the D band) depends directly on the number of defects. In this case, however, the relative intensity of the bands associated with the Raman DR components varies from one sample to another. This band has also been studied in other  $sp^2$  carbon materials such as carbon nanotubes (Shimada et al., 2005). Based on what was observed in this work, it could be inferred that the intensity of this band is affected by the transfer process, which could have to do with the substrate change or with the increase of the defects of the material. However, experimental and theoretical support is still needed to be able to correctly predict its behavior. Finally, it is important to highlight that the most recent bibliographic review studies on Raman spectroscopy of graphene do not mention anything about this peak, even though in the spectra they include, it does appear (Nanda et al., 2016).

Figure 6. Raman spectra of three graphene samples synthesized at different conditions on copper (black line) and then transferred to silicon (red line).



In general, to synthesize graphene with 4 to 6 layers it was possible to narrow the values for the 4 parameters studied in the synthesis. It is advisable to use the lowest possible precursor flow since the objective is to obtain few layers of material. This value is restricted by the minimum flow that the mass flow controller allows to be programmed. In this case the minimum value that can be programmed is 3 sccm. When adding a flow lower than 3 sccm the device error increases significantly. For this reason, 3 sccm was chosen as the optimal  $CH_4$  flow. On the other hand, with respect to the  $H_2$  flow, by consensus between the results obtained and the information found in the literature it was concluded that it is possible to synthesize graphene in the absence of  $H_2$ . However, the most advisable is to add a small amount so that the synthesized material presents better structural properties, lower number of defects, and grains of larger area. Therefore, it was

decided to add 5 sccm of hydrogen in all the syntheses. With respect to the synthesis time, the best results were obtained with 3 and 10 minutes. However, it was decided that the most adequate synthesis time is 10 minutes since the number of layers formed is the same as when using 3 minutes, but the sheets may be better finished and with fewer defects. Finally, as synthesis temperature 950 °C or 1000 °C can be used. With both temperatures in combination with the parameters mentioned previously graphene between 4 and 6 layers can be obtained to subsequently transfer it. Lastly, it is important to highlight again that to achieve an efficient transfer of 1 to 2 layers of graphene it is advisable to prepare a sample that presents 4 to 6 layers on the original substrate.

## 4. CONCLUSIONS

In this work the synthesis of graphene by CVD on copper was systematically investigated employing two carbon precursors ( $\text{CH}_4$  and  $\text{C}_2\text{H}_2$ ) and varying synthesis time, temperature, precursor flow, and hydrogen. It was found that methane ( $\text{CH}_4$ ) allows a more reproducible control of the number of layers and leads to sheets with a lower density of defects in comparison with acetylene ( $\text{C}_2\text{H}_2$ ), which favors rapid growth but is difficult to control and presents greater structural disorder. The transfer process (PMMA + Cu etch) induces an effective reduction of the number of layers (4–6 layers on Cu → 1–2 layers after transfer) and modifies Raman characteristics associated with double resonances, which suggests that partial exfoliation, the effect of the substrate, and PMMA residues influence the observed spectroscopy. From the optimizations, the recommended working condition is:  $\text{CH}_4$  at 950–1000 °C, minimum compatible precursor flow (3 sccm in the system used), 5 sccm of  $\text{H}_2$ , and a time of 10 min to obtain transferable sheets of 1–2 layers after transfer. Finally, to strengthen the results and move toward applications, it is necessary to complement this study with TEM/AFM characterization of edges, and a post-transfer cleaning protocol that reduces PMMA residues and process variability.

## REFERENCES

- Balandin, A. A., Ghosh, S., Bao, W., Calizo, I., Teweldebrhan, D., Miao, F., & Lau, C. N. (2008). Superior thermal conductivity of single-layer graphene. *Nano Letters*, 8(3), 902–907. <https://doi.org/10.1021/nl0731872>
- Coraux, J., N'Diaye, A. T., Engler, M., Busse, C., Wall, D., Buckanie, N., Meyer zu Heringdorf, F. J., Van Gastel, R., Poelsema, B., & Michely, T. (2009). Growth of graphene on Ir(111). *New Journal of Physics*, 11, Article 023006. <https://doi.org/10.1088/1367-2630/11/2/023006>
- Ferrari, A. C., Meyer, J. C., Scardaci, V., Casiraghi, C., Lazzeri, M., Mauri, F., Piscanec, S., Jiang, D., Novoselov, K. S., Roth, S., & Geim, A. K. (2006). Raman spectrum of graphene and graphene layers. *Physical Review Letters*, 97(18), Article 187401. <https://doi.org/10.1103/PhysRevLett.97.187401>

- First, P. N., de Heer, W. A., Seyller, T., Berger, C., Joseph, A., & Moon, J. (2010). Epitaxial graphenes on silicon carbide. *MRS Bulletin*, 35(4), 296–305. <https://doi.org/10.1557/mrs2010.552>
- Gao, E., Lin, S. Z., Qin, Z., Buehler, M. J., Feng, X. Q., & Xu, Z. (2018). Mechanical exfoliation of two-dimensional materials. *Journal of the Mechanics and Physics of Solids*, 115, 248–262. <https://doi.org/10.1016/j.jmps.2018.03.014>
- Ghosh, S., Bao, W., Nika, D. L., Subrina, S., Pokatilov, E. P., Lau, C. N., & Balandin, A. A. (2010). Dimensional crossover of thermal transport in few-layer graphene. *Nature Materials*, 9(7), 555–558. <https://doi.org/10.1038/nmat2753>
- Güler, Ö., & Bağcı, N. (2020). A short review on mechanical properties of graphene reinforced metal matrix composites. *Journal of Materials Research and Technology*, 9(6), 6808–6833. <https://doi.org/10.1016/j.jmrt.2020.01.077>
- Kamedulski, P., Ilnicka, A., Łukaszewicz, J. P., & Skorupska, M. (2019). Highly effective three-dimensional functionalization of graphite to graphene by wet chemical exfoliation methods. *Adsorption*, 25(3), 631–638. <https://doi.org/10.1007/s10450-019-00067-9>
- Karu, A. E., & Beer, M. (1966). Pyrolytic formation of highly crystalline graphite films. *Journal of Applied Physics*, 37(5), 2179–2181. <https://doi.org/10.1063/1.1708759>
- Kwon, S. Y., Ciobanu, C. V., Petrova, V., Shenoy, V. B., Bareño, J., Gambin, V., Petrov, I., & Kodambaka, S. (2009). Growth of semiconducting graphene on palladium. *Nano Letters*, 9(12), 3985–3990. <https://doi.org/10.1021/nl902140j>
- Lee, C., Wei, X., Kysar, J. W., & Hone, J. (2008). Measurement of the elastic properties and intrinsic strength of monolayer graphene. *Science*, 321(5887), 385–388. <https://doi.org/10.1126/science.1157996>
- Li, X., Cai, W., An, J., Kim, S., Nah, J., Yang, D., Piner, R., Velamakanni, A., Jung, I., Tutuc, E., Banerjee, S. K., Colombo, L., & Ruoff, R. S. (2009). Large-area synthesis of high-quality and uniform graphene films on copper foils. *Science*, 324(5932), 1312–1314. <https://doi.org/10.1126/science.1171245>
- Liu, M., Zhang, X., Wu, W., Liu, T., Liu, Y., Guo, B., & Zhang, R. (2019). One-step chemical exfoliation of graphite to ~100% few-layer graphene with high quality and large size at ambient temperature. *Chemical Engineering Journal*, 355, 181–185. <https://doi.org/10.1016/j.cej.2018.08.146>
- Liu, N., Luo, F., Wu, H., Liu, Y., Zhang, C., & Chen, J. (2008). One-step ionic-liquid-assisted electrochemical synthesis of ionic-liquid-functionalized graphene sheets directly from graphite. *Advanced Functional Materials*, 18(10), 1518–1525. <https://doi.org/10.1002/adfm.200700797>
- Malard, L. M., Pimenta, M. A., Dresselhaus, G., & Dresselhaus, M. S. (2009). Raman spectroscopy in graphene. *Physics Reports*, 473(5–6), 51–87. <https://doi.org/10.1016/j.physrep.2009.02.003>
- Martini, L., Chen, Z., Mishra, N., Barin, G. B., Fantuzzi, P., Ruffieux, P., Fasel, R., Feng, X., Narita, A., Coletti, C., Müllen, K., & Candini, A. (2019). Structure-dependent electrical properties of graphene nanoribbon devices with graphene electrodes. *Carbon*, 146, 36–43. <https://doi.org/10.1016/j.carbon.2019.01.071>
- Nair, R. R., Blake, P., Grigorenko, A. N., Novoselov, K. S., Booth, T. J., Stauber, T., Peres, N. M. R., & Geim, A. K. (2008). Fine structure constant defines visual transparency of graphene. *Science*, 320(5881), 1308. <https://doi.org/10.1126/science.1156965>
- Nanda, S. S., Kim, M. J., Yeom, K. S., An, S. S. A., Ju, H., & Yi, D. K. (2016). Raman spectrum of graphene with its versatile future perspectives. *TrAC Trends in Analytical Chemistry*, 80, 125–131. <https://doi.org/10.1016/j.trac.2016.02.024>



- Ni, Z., Wang, Y., Yu, T., & Shen, Z. (2008). Raman spectroscopy and imaging of graphene. *Nano Research*, 1(4), 273–291. <https://doi.org/10.1007/s12274-008-8036-1>
- Novoselov, K. S., Fal'ko, V. I., Colombo, L., Gellert, P. R., Schwab, M. G., & Kim, K. (2012). A roadmap for graphene. *Nature*, 490(7419), 192–200. <https://doi.org/10.1038/nature11458>
- Olabi, A. G., Ali, M., Wilberforce, T., & Taha, E. (2021). Application of graphene in energy storage device – A review. *Renewable and Sustainable Energy Reviews*, 135, 110026. <https://doi.org/10.1016/j.rser.2020.110026>
- Pimenta, M. A.; Dresselhaus, G.; Dresselhaus, M. S.; Cançado, L. G.; Jorio, A.; Saito, R. (2007). Studying Disorder in Graphite-Based Systems by Raman Spectroscopy. *Phys. Chem. Chem. Phys.* 9 (11), 1276–1291. <https://doi.org/10.1039/b613962k>
- Qi, M., Ren, Z., Jiao, Y., Zhou, Y., Xu, X., Li, W., Li, J., Zheng, X., & Bai, J. (2013). Hydrogen kinetics on scalable graphene growth by atmospheric pressure chemical vapor deposition with acetylene. *Journal of Physical Chemistry C*, 117(27), 14348–14353. <https://doi.org/10.1021/jp403410b>
- Saito, K., Nakamura, J., & Natori, A. (2007). Ballistic thermal conductance of a graphene sheet. *Physical Review B*, 76(11), 1–4. <https://doi.org/10.1103/PhysRevB.76.115409>
- Saito, R., Hofmann, M., Dresselhaus, G., Jorio, A., & Dresselhaus, M. S. (2011). Raman spectroscopy of graphene and carbon nanotubes. *Advances in Physics*, 60(3), 413–550. <https://doi.org/10.1080/0018732.2011.582251>
- Segura, R. A., Olivares, F., Maze, J., Häberle, P., Henríquez, R. (2016). Photoelectrochemical Activity of Graphene Supported Titanium Dioxide. *Journal of Nanomaterials*, 7914189, 1-6. <http://dx.doi.org/10.1155/2016/7914189>
- Shimada, T., Sugai, T., Fantini, C., Souza, M., Cançado, L. G., Jorio, A., Pimenta, M. A., Saito, R., Grüneis, A., Dresselhaus, G., Dresselhaus, M. S., Ohno, Y., Mizutani, T., & Shinohara, H. (2005). Origin of the 2450 cm<sup>-1</sup> Raman bands in HOPG, single-wall and double-wall carbon nanotubes. *Carbon*, 43(5), 1049–1054. <https://doi.org/10.1016/j.carbon.2004.11.044>
- Song, W., Jeon, C., Kim, S. Y., Kim, Y., Kim, S. H., Lee, S. I., Jung, D. S., Jung, M. W., An, K. S., & Park, C. Y. (2014). Two selective growth modes for graphene on a Cu substrate using thermal chemical vapor deposition. *Carbon*, 68, 87–94. <https://doi.org/10.1016/j.carbon.2013.10.039>
- Suk, J. W., Kitt, A., Magnuson, C. W., Hao, Y., Ahmed, S., An, J., Swan, A. K., Goldberg, B. B., & Ruoff, R. S. (2011). Transfer of CVD-grown monolayer graphene onto arbitrary substrates. *ACS Nano*, 5(9), 6916–6924. <https://doi.org/10.1021/nn201207c>
- Vlassiuk, I., Regmi, M., Fulvio, P., Dai, S., Datskos, P., Eres, G., & Smirnov, S. (2011). Role of hydrogen in chemical vapor deposition growth of large single-crystal graphene. *ACS Nano*, 5(7), 6069–6076. <https://doi.org/10.1021/nn201978y>
- Wei, D., Liu, Y., Wang, Y., Zhang, H., Huang, L., & Yu, G. (2009). Synthesis of N-doped graphene by chemical vapor deposition and its electrical properties. *Nano Letters*, 9(5), 1752–1758. <https://doi.org/10.1021/nl803279t>
- Yu, Q., Lian, J., Siriponglert, S., Li, H., Chen, Y. P., & Pei, S. S. (2008). Graphene segregated on Ni surfaces and transferred to insulators. *Applied Physics Letters*, 93(11), 1–4. <https://doi.org/10.1063/1.2982585>
- Zhang, W., Wu, P., Li, Z., & Yang, J. (2011). First-principles thermodynamics of graphene growth on Cu surfaces. *Journal of Physical Chemistry C*, 115(36), 17782–17787. <https://doi.org/10.1021/jp2006827>

## ABOUT THE ORGANIZER

**Emilio Castro Otero** é professor da área de Bioengenharia na *Universitat Internacional de Catalunya*, Barcelona, Espanha. Pesquisador com ampla trajetória científica nas áreas de biomateriais, nanotecnologia, química física de polímeros e sistemas nanoestruturados aplicados à medicina regenerativa e à liberação controlada de fármacos. Sua produção abrange estudos fundamentais sobre auto-organização molecular, interações entre copolímeros e surfactantes, estabilidade proteica e desenvolvimento de nanopartículas e hidrogéis inteligentes, contribuindo de maneira significativa para a compreensão dos mecanismos físico-químicos que governam materiais avançados e sua aplicabilidade biomédica. Seu trabalho mais recente, publicado em *Acta Biomaterialia* (2023), aborda o papel angiogênico e imunomodulador de íons nas fases iniciais da regeneração óssea, consolidando sua atuação no campo dos biomateriais bioativos. Ao longo de sua carreira, publicou artigos de impacto em periódicos como *Langmuir*, *Biomacromolecules*, *Journal of Biomedical Nanotechnology*, *Macromolecular Bioscience*, *Journal of Physical Chemistry B*, *Chemical Physics* e *Journal of Colloid and Interface Science*, além de contribuir com capítulo de livro na área de nanomedicina, ampliando sua presença internacional na literatura científica.

Entre suas contribuições relevantes, destacam-se estudos sobre auto-organização de elastina recombinante e copolímeros responsivos à temperatura, síntese e caracterização de nanopartículas funcionalizadas, incluindo magnetita pegulada e nanocápsulas multifuncionais, e sistemas poliméricos capazes de encapsular e liberar fármacos de forma controlada, com foco em aplicações oncológicas e terapêuticas avançadas. Sua pesquisa também inclui extensas investigações termodinâmicas envolvendo surfactantes, copolímeros e sistemas micelares complexos, bem como análises detalhadas de interações entre proteínas e fármacos anfífilicos, contribuindo para o entendimento de processos de dobramento, estabilidade e agregação proteica. Com forte perfil interdisciplinar, o pesquisador tem colaborado com grupos internacionais de renome em bioengenharia, físico-química de materiais, nanotecnologia e biotecnologia aplicada, contribuindo para o desenvolvimento de estratégias inovadoras em engenharia de tecidos, medicina regenerativa e materiais biomiméticos.

Ao longo de quase duas décadas de produção científica contínua, Emilio Castro Otero consolidou uma carreira marcada pela investigação rigorosa, inovação metodológica e abordagem integrada da ciência dos materiais, oferecendo contribuições relevantes tanto para o avanço do conhecimento fundamental quanto para o desenvolvimento de soluções tecnológicas com potencial translacional na área biomédica.

ORCID: <https://orcid.org/0000-0002-7491-4169>

## INDEX

### A

Adsorption 13, 80, 96, 97, 98, 100, 101, 102, 103, 104, 105

Aerografia 15, 16, 17, 18, 21, 22, 23, 25, 26, 27

Antiseptics 86, 87

Arsenic 96, 97, 98, 99, 100, 101, 102, 103, 104, 105

### B

Bactericidal 86, 87

Blood vessel 75, 84

### C

Chemical vapor deposition 1, 14

Conductive hydrogel 75

Cromo 50, 51, 53, 54, 58, 59

Cucurbita moschata 60, 61, 62, 63, 68, 70, 71, 72, 73

### E

Electrodeposición 50, 51, 52, 53, 54, 55, 56

Emulsions 61, 63, 64, 73

### F

Fiação por Sopro de Solução 16, 22, 24, 30

### G

Graphene 1, 2, 3, 4, 5, 6, 7, 8, 9, 10, 11, 12, 13, 14, 27, 31, 34, 35

Graphene transfer 1, 4, 9

Groundwater 96, 97, 98, 99, 105

### I

Inflammatory breast neoplasms 61

Iron nanoparticles 96, 100, 101, 104, 105

Iron oxide 96, 97, 100, 101, 102, 104, 105

## L

Low-cost filter 96

## M

Morfología 22, 24, 33, 47, 51, 53, 56, 57

## N

Nanocompuesto 34, 36, 37, 38, 43, 47

Nanofibras 15, 16, 17, 18, 19, 20, 21, 22, 24, 25, 26, 27, 30, 32

Nanoparticles 32, 35, 51, 62, 69, 72, 74, 75, 77, 78, 80, 81, 82, 83, 85, 86, 87, 88, 89, 90, 91, 92, 93, 94, 96, 97, 100, 101, 102, 103, 104, 105

Nanopartículas de óxidos metálicos 34

Nanopartículas metálicas 51, 52

## O

Óxido de grafeno 34, 36, 39, 40, 48, 49

## P

PEDOT nanoparticles 74, 75, 77, 78, 81, 82, 83

Propiedades poliméricas 16

## R

Raman spectroscopy 1, 5, 11, 13, 14, 35

Recubrimientos nanoestructurados 50, 51, 53, 59

## S

Sensores de gas 34, 36

Smooth muscle cells 74, 75, 82, 84

## T

Toxicity tests 61

Tratamento de água 15, 16, 17, 18, 25, 26

## V

Vascular regeneration 74, 75, 83

Virucidal and bioactive compounds 86

